

High Electrical Spectral Efficiency Silicon Photonic Receiver with Carrier-Assisted Differential Detection

Jingchi Li¹, Zhen Wang¹, Honglin Ji², Xingfeng Li¹, Haoshuo Chen³, Ranjith Rajasekharan Unnithan², William Shieh², and Yikai Su^{1,*}

¹State Key Laboratory of Advanced Optical Communication Systems and Networks, Department of Electronic Engineering, Shanghai Jiao Tong University, 800 Dongchuan Rd, Shanghai, 200240, China

²Department of Electrical and Electronic Engineering, The University of Melbourne, Parkville, VIC 3010, Australia

³Nokia Bell Labs, 600 Mountain Ave, Murray Hill, NJ 07974, USA

Author e-mail address: yikaisu@sjtu.edu.cn

Abstract: We experimentally demonstrate a silicon photonic carrier-assisted differential detection receiver with a single-polarization 224-Gb/s 16-QAM signal transmitted through 80-km SMF. For an integrated direct detection receiver with transmission demonstration, we achieve the highest electrical spectral efficiency/# of polarizations of 6.4 (net 4.6) b/s/Hz. © 2022 The Authors

1. Introduction

The demand for cost-effective high-speed solutions in short-reach optical communications has increased dramatically. Although coherent detection is capable of field recovery and has superior performance [1], the high hardware complexity and requirement on costly narrow-linewidth local oscillator (LO) hinder its applications. On the other hand, direct detection (DD) with a simpler structure remains a dominant solution in cost-sensitive short-reach systems. However, conventional DD suffers from chromatic dispersion (CD). Single sideband-self-coherent detection (SSB-SCD) was then proposed to deal with the CD impacts but with a limited electrical spectral efficiency (ESE). Recently, an advanced DD scheme called carrier-assisted differential detection (CADD) [2] was proposed. The CADD can recover the optical field of complex-valued double sideband (DSB) signals with a receiver bandwidth of approximately half of the baud rate, realizing a higher ESE than both conventional DD and SSB-SCD. Moreover, the CADD is a LO-free scheme, which greatly saves the implementation cost and makes it well-positioned for integration.

In this paper, we demonstrate a silicon photonic (SiP) CADD receiver for the first time. The cost and power consumption are reduced compared with the SiP coherent receivers [3, 4], since it saves a LO and avoids the sophisticated wavelength alignment between Tx and Rx lasers. Compared with the SiP DD receivers [5-10], the SiP CADD receiver achieves a higher ESE due to the capability of recovering complex-valued DSB signals. A review of integrated DD receivers with transmission results is provided in Fig. 1. With a 35-GHz single polarization SiP CADD receiver, we successfully transmit a 224-Gb/s (162-Gb/s net rate) orthogonal frequency division multiplexing (OFDM) 16-ary quadrature amplitude modulation (16-QAM) signal over 80-km single-mode fiber (SMF). The ESE is 6.4 (net ESE of 4.6) b/s/Hz. To the best of our knowledge, we achieve the highest ESE/# of polarizations for a SiP DD receiver with transmission demonstration.

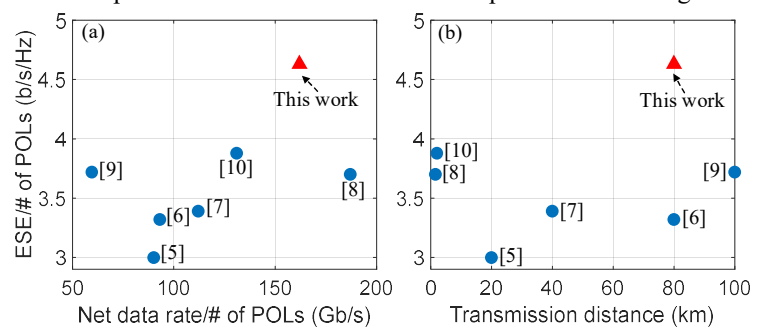


Fig. 1. Review of integrated DD receivers. (a) ESE/# of polarizations (POLs) vs. Net data rate/# of POLs. (b) ESE/# of POLs vs. Transmission distance.

With a 35-GHz single polarization SiP CADD receiver, we successfully transmit a 224-Gb/s (162-Gb/s net rate) orthogonal frequency division multiplexing (OFDM) 16-ary quadrature amplitude modulation (16-QAM) signal over 80-km single-mode fiber (SMF). The ESE is 6.4 (net ESE of 4.6) b/s/Hz. To the best of our knowledge, we achieve the highest ESE/# of polarizations for a SiP DD receiver with transmission demonstration.

2. Operation principle

Fig. 2(a) depicts the schematic of the CADD receiver, which can reconstruct the field of complex-valued DSB signal through the beating between the received signal and its delayed version [2]. Fig. 2(b) presents the structure of the integrated CADD receiver. The optical signal is coupled into the silicon chip using a grating coupler, and split into two branches with one input to a 90° optical hybrid and the other delayed for differential detection. Here, the delay parameter is designed to be 111 ps for a proper multiband allocation considering the system bandwidth limitation. A 4×4 multimode interferometer (MMI) functions as a 90° optical hybrid. One branch of the delayed signals is detected with a single-ended photodiode (PD) and the other is input to the hybrid. The outputs of the 4×4 MMI are fed into four single-ended PDs, which are properly combined to provide balanced detection. Finally, three detected electrical signals are collected using high-speed probes and captured with a digital scope. Fig. 2(c) shows the micrograph of

the integrated CADD receiver fabricated on a silicon-on-insulator (SOI) wafer with a 220-nm-thick silicon layer. The footprint is $\sim 1.1 \text{ mm} \times 0.9 \text{ mm}$. The insets (i-iii) illustrate the magnified micrographs of the bending, 90° optical hybrid (4×4 MMI), and PD, respectively. The reported bandwidth of the on-chip germanium PD is 21 GHz with a -1-V bias voltage and 33 GHz with a -3-V bias voltage, respectively. Aiming for a high-rate transmission, we set the bias voltage to -3 V in the experiment. This integrated CADD receiver operates with a single polarization due to the use of the grating coupler. To realize a dual-polarization CADD receiver, an edge coupler, a dynamic polarization rotator, a polarization beam splitter and two single-polarization CADD receivers are required on a chip.

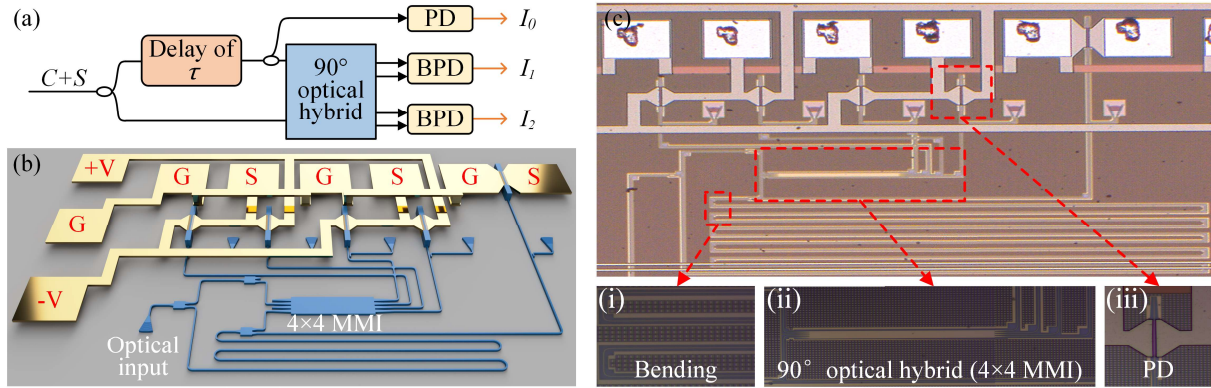


Fig. 2 (a) Schematic of the CADD receiver. (b) Structural illustration and (c) micrograph of the integrated CADD receiver chip. Insets (i-iii) magnified micrographs of the bending, 90° optical hybrid (4×4 MMI), and PD, respectively.

3. Experimental setup and results

The experimental setup is presented in Fig. 3. At the transmitter side, the OFDM 16-QAM signal is generated using a 100-GSa/s digital-to-analog converter (DAC) (Micram DAC4). A continuous light from a 100-kHz external cavity laser (ECL) is boosted and split into two branches for the generation of a signal and a carrier. The input optical power to an IQ modulator biased at its transmission null is 15 dBm. A variable optical attenuator (VOA) is placed in the carrier path to adjust the carrier-to-signal power ratio (CSPR). With two polarization controllers (PC) and a polarizer, the polarization states between the modulated signal and the carrier are aligned. The output power of the polarizer is -4 dBm . At the receiver side, a VOA is utilized to vary the received optical power (ROP). Then, after being amplified by an erbium doped fiber amplifier (EDFA), the signal is received with the integrated CADD receiver. In the experiment, we kept the silicon chip input power at 16.5 dBm. Finally, the detected signals are read out with probes and captured using a digital storage oscilloscope (DSO) (LeCroy 36Zi-A) operating at 80 GSa/s.

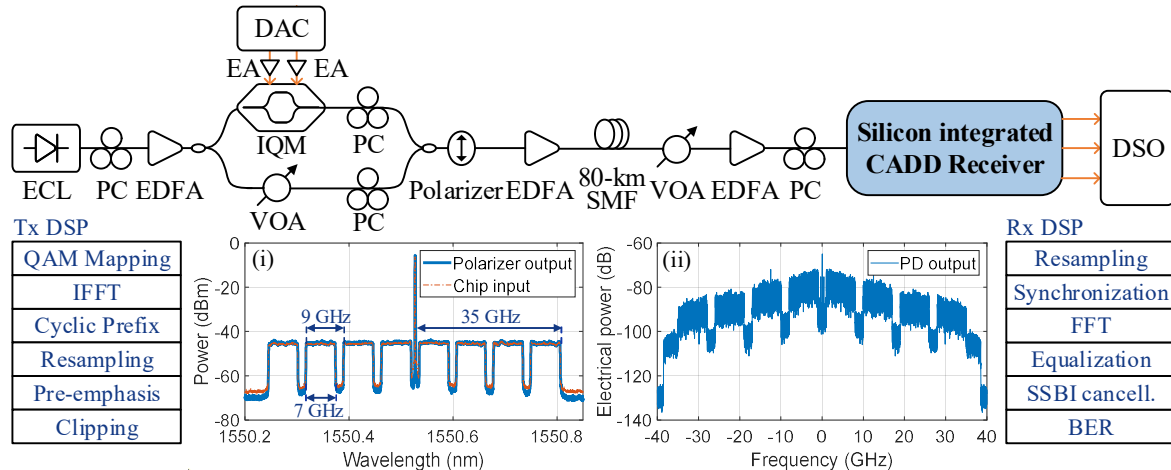


Fig. 3 Experimental setup and the DSP flow charts. Inset (i) optical spectra at different stages in the transmission case. Inset (ii) electrical spectrum of the signal monitored by single-ended PD in the integrated CADD receiver.

The digital signal processing (DSP) flow charts are also shown in Fig. 3. For transmitter DSP, the binary data is mapped to the 16-QAM symbol and the OFDM-modulated signal is generated with a 4096-size fast *Fourier* transform

(IFFT). 2864 subcarriers are filled with data. In the experiment, we generated an 8-band loaded OFDM 16-QAM signal: each band occupies 7 GHz and a 2-GHz guard band is inserted between two sub-bands. The guard band is essential to prevent severe signal-signal beat interference (SSBI) enhancement caused by the transmission nulls of filter response originated from the delay line and the optical hybrid. The inset (i) plots the optical spectra at different stages. Pre-emphasis technique is employed for high-frequency attenuation compensation. The system information rate is 224-Gb/s with a 35-GHz required receiver bandwidth. After being clipped to a 10-dB peak-to-average power ratio (PAPR), the signal is loaded into the DAC. In the receiver DSP, the captured signals are synchronized and combined. The inset (ii) illustrates the electrical spectrum of the signal monitored by on-chip single-ended PD. The high-frequency roll-off mainly results from the bandwidth limitations of the PD, the high-speed probe, and the cable connecting the probe and the DSO. The spikes at -12.5 GHz and 12.5 GHz are the clock leakages of the DAC. For signal reconstruction, equalization and SSBI iterative cancellation algorithm are employed [2], followed by the bit error ratio (BER) calculation.

Fig. 4 presents the experimental results. CSPR is a key parameter in the CADD receiver: a high CSPR contributes to a large desired linear term whereas sacrifices the effective signal power. It can be observed that the optimal CSPR value is 12 dB for the two cases. Fig. 4(b) depicts the BER versus the number of iterations of the SSBI cancellation algorithm in the OBTB case. Two-times iteration is sufficient to remove the SSBI effectively. Fig. 4(c) presents the BER versus ROP in the OBTB case and after the 80-km transmission. In the OBTB case, the carrier-assisted complex-valued DSB signal output by the polarizer is directly input to the VOA at the receiver. In the transmission case, the signal is boosted to a launch power of 6 dB using an EDFA and launched into an 80-km SMF for transmission. A transmission sensitivity penalty can be observed in Fig. 4(c). The penalty is attributed to the facts that the EDFA in the transmitter introduces excess amplified spontaneous emission (ASE) noise and the CD results in a higher PAPR. After the 80-km transmission with the 224-Gb/s OFDM 16-QAM signal, the BER is below the 25% soft-decision forward error correction (SD-FEC) threshold [11]. The insets (i-ii) show the constellations of 16-QAM signal in the OBTB case at -4 -dB ROP and in the transmission case at -9 -dB ROP, respectively.

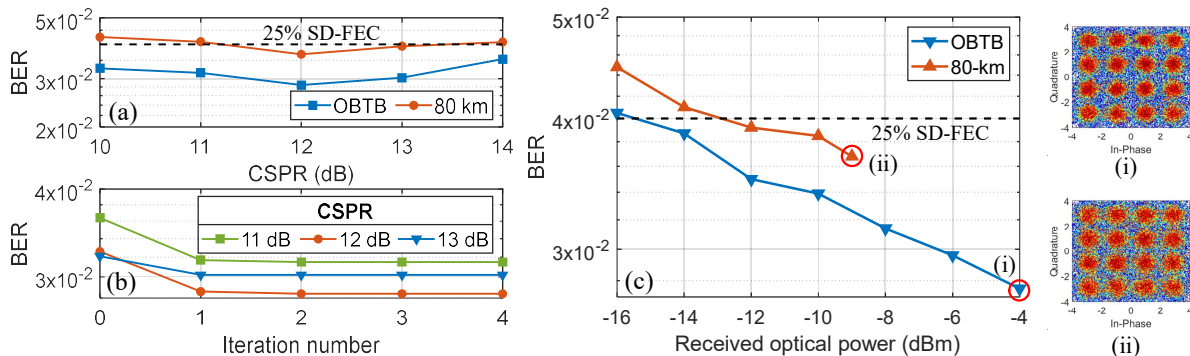


Fig. 4. (a) BER vs. CSPR in the OBTB and transmission cases. (b) BER vs. iteration number of SSBI cancellation algorithm in the OBTB case. (c) BER as a function of ROP in the OBTB case and after the 80-km transmission. Insets (i-ii) constellations in the OBTB case at -4 -dB ROP and in the transmission case at -9 -dB ROP, respectively.

4. Conclusion

We have demonstrated single-polarization 224-Gb/s complex-valued DSB 16-QAM signal transmission over 80-km SMF with a 35-GHz SiP CADD receiver. The SiP CADD receiver is fully complementary-metal-oxide-semiconductor (CMOS) compatible in fabrication. Moreover, the elimination of the narrow linewidth LO and the low electrical bandwidth requirement effectively reduce the hardware complexity and cost. To the best of our knowledge, this is the first single-polarization SiP DD receiver which can recover the optical field of complex-valued DSB signals, and we achieve the highest 6.4 (net 4.6)-b/s/Hz ESE/# of polarizations for an integrated DD receiver with transmission demonstration. As such, we believe that our LO-free SiP receiver has a great potential for future cost-effective passive optical network (PON), data center interconnect, and mobile front haul applications.

5. References

- [1] K. Kikuchi, *J. Lightw. Technol.*, **34**, 157–179 (2016).
- [2] W. Shieh, *et al.*, *Light: Sci. Appl.*, **9**, 1–9 (2020).
- [3] P. Dong, *et al.*, in *Proc. OFC/NFOEC'2013*, paper PDP5C.6.
- [4] Y. Wang, *et al.*, *Nature. Comm.*, **12**, 5076 (2021).
- [5] P. Dong, *et al.*, *J. Lightw. Technol.*, **34**, 79–84 (2016).
- [6] Y. Tong, *et al.*, *J. Lightw. Technol.*, **37**, 3532–3538 (2019).
- [7] S. Zhang, *et al.*, *OFC'2021*, paper W7F.4.
- [8] D. W. U. Chan, *et al.*, *J. Lightw. Technol.*, Early Access (2022).
- [9] P. Dong, *et al.*, *Opt. Exp.*, **24**, 14208–14214 (2016).
- [10] Y. Hong, *et al.*, *J. Lightw. Technol.*, **39**, 1138–1147 (2021).
- [11] L. Schmalen, *et al.*, *J. Lightw. Technol.*, **33**, 1109–1116 (2015).